

Communication

Preparation Strategy Using Pre-Nucleation Coupled with In Situ Reduction for a High-Performance Catalyst towards Selective Hydrogen Production from Formic Acid

Qinglei Meng^{1,2,3}, Xiaolong Yang^{1,2,3}, Xian Wang^{1,2,3}, Meiling Xiao^{2,4}, Kui Li^{1,3} , Zhao Jin^{1,2,3,4}, Junjie Ge^{1,2,3,4,*}, Changpeng Liu^{1,2,3,4,*}  and Wei Xing^{1,2,3,4,*}

- ¹ Laboratory of Advanced Power Sources, Changchun Institute of Applied Chemistry, Chinese Academy of Sciences, Changchun 130022, China; qlmeng@ciac.ac.cn (Q.M.); xlyang@ciac.ac.cn (X.Y.); xwang@ciac.ac.cn (X.W.); kui.li@yahoo.com (K.L.); zjin@ciac.ac.cn (Z.J.)
- ² School of Applied Chemistry and Engineering, University of Science and Technology of China, Hefei 230026, China; mxiao@ciac.ac.cn
- ³ Jilin Province Key Laboratory of Low Carbon Chemical Power Sources, Changchun Institute of Applied Chemistry, Chinese Academy of Sciences, Changchun 130022, China
- ⁴ State Key Laboratory of Electroanalytical Chemistry, Changchun Institute of Applied Chemistry, Chinese Academy of Sciences, Changchun 130022, China
- * Correspondence: gejj@ciac.ac.cn (J.G.); liuchp@ciac.ac.cn (C.L.); xingwei@ciac.ac.cn (W.X.)

Abstract: Formic acid decomposition (FAD) is one of the most promising routes for rapid hydrogen (H₂) production. Extensive efforts have been taken to develop efficient catalysts, which calls for the simultaneous regulation of the electronic structure and particle size of the catalyst. The former factor determines the intrinsic performance, while the latter corresponds to the active site utilization. Here, an effective preparation strategy, pre-nucleation coupled with in situ reduction, is developed to realize and well-tune both surface electronic states and particle size of the palladium (Pd) catalyst. Benefiting from the structural merits, the as-prepared catalyst exhibits high mass-specific activity of 8.94 mol_{H₂}/(g_{Pd}·h) with few carbon monoxide (CO) molecules, and the activation energy could reach a value as small as 33.1 kJ/mol. The work not only affords a highly competitive FAD catalyst but also paves a new avenue to the synthesis of ultra-fine metal nanoparticles with tailorable electronic structures.

Keywords: hydrogen evolution; formic acid; heterogeneous catalysis; high selectivity; Pd-PdO interface



Citation: Meng, Q.; Yang, X.; Wang, X.; Xiao, M.; Li, K.; Jin, Z.; Ge, J.; Liu, C.; Xing, W. Preparation Strategy Using Pre-Nucleation Coupled with In Situ Reduction for a High-Performance Catalyst towards Selective Hydrogen Production from Formic Acid. *Catalysts* **2022**, *12*, 325. <https://doi.org/10.3390/catal12030325>

Academic Editor: José Antonio Calles

Received: 9 February 2022

Accepted: 9 March 2022

Published: 11 March 2022

Publisher's Note: MDPI stays neutral with regard to jurisdictional claims in published maps and institutional affiliations.



Copyright: © 2022 by the authors. Licensee MDPI, Basel, Switzerland. This article is an open access article distributed under the terms and conditions of the Creative Commons Attribution (CC BY) license (<https://creativecommons.org/licenses/by/4.0/>).

1. Introduction

Hydrogen energy has been considered one of the most promising energy carriers in the future of the energy system, as it could provide large energy (120 MJ/kg) [1] without furthering climate issues because of its clean products [2,3]. However, increasingly strict and harsh demand have been increased regarding hydrogen storage and transportation along with the rapid development of hydrogen energy [4], as hydrogen gas is inflammable, explosive, and not easily compressed. To make hydrogen storage and transportation safer and more efficient, hydrogen production from small organic molecules has been suggested as it could stay in a liquid form and the process has a higher hydrogen capacity than the traditional methods [5,6]. In addition, the hydrogen gas produced from those molecules could be utilized using a series, such as the proton exchange membrane fuel cell (PEMFC), which could transfer the energy into electrical energy directly and efficiently. To realize the application of the hydrogen supplement from molecules, the environment of hydrogen production should be mild enough to make it easy to popularize.

Formic acid decomposition has been considered one of the most suggested pathways for the mobile supplement of hydrogen gas [7], as it is the only molecular mechanism that

could provide hydrogen gas fast at room temperature, along with a competitive hydrogen capacity ($0.057 \text{ kg}_{\text{H}_2}/\text{L}$), and is the only organic molecule that can be decomposed at ambient temperatures [8]. Because of these advantages, formic acid decomposition has attracted much attention, so there have been a number of reports about the mechanism of the dehydrogenation pathways and the preparation of high-performance catalysts for formic acid decomposition. Though the dehydrogenation pathway of formic acid decomposition is still in dispute, as the density functional theory (DFT) calculations confirm the H-down mode [9], while experiments about catalysts always adopt the H-up mode [10], there has been a consensus that the Pd(II) could boost the performance of the prepared catalyst [11–13], from which the confirmation of the promoting effect of the break of C-H bonds has been reported. The mainstream reported catalyst has always emphasized the effect of Pd(II) on the high performance and low CO yield. To keep the Pd(II) content in the catalyst high, traditional methods mainly focus on the dopant in both the support and the catalyst, such as the nitrogen (N)-doped C for the support of Pd [14–18] and alloying to form palladium gold alloy (PdAu), palladium silver alloy (PdAg), and palladium nickel alloy (PdNi) [19–25] for formic acid decomposition. However, Pd(II) is the oxidized form of Pd, which is easily reduced during the preparation of the catalyst by multifarious reducing agents such as sodium borohydride (NaBH_4), ethylene glycol (EG), and H_2 . To inhibit the over-reduction during the reduction of Pd, the in situ reduction method has been suggested, a process that uses the formic acid and formate as the reducing agent [26]. This reducing agent could reduce the catalyst to the most suitable surface electronic structure for the reaction. However, there are still problems with this method as the size of the particles could not be as small as the catalysts prepared by the traditional methods, since the reducibility of formic acid and formate is mainly dependent on formic acid. Therefore, it is difficult to carry out the reduction in an alkaline environment, as well as for the nucleation of Pd in an acidic environment as the Pd atom is always protected by chlorine (Cl) and other ligands existing as PdCl_4^{2-} or in other forms. The slow nucleation of the in situ reduction makes the particles too large to compete with the catalysts prepared by other methods, though it has the most suitable electronic structure.

To optimize the in situ reduction preparation of the small-size nanoparticles with suitable electronic structures, the pre-nucleation pathway is adopted in this work. The aim of this method is to use the in situ reduction only to adjust the surface electronic structure and to leave the control of the particle size to the pre-nucleation. In this way, the catalyst with both the small particle size and the suitable surface electronic structure could be prepared, which could exhibit excellent performance to the Pd/C catalysts prepared by the traditional method [27] and could exhibit competitive performance to many catalysts prepared by the doped method such as N-doped [28], boron(B)-doped [29], and so on.

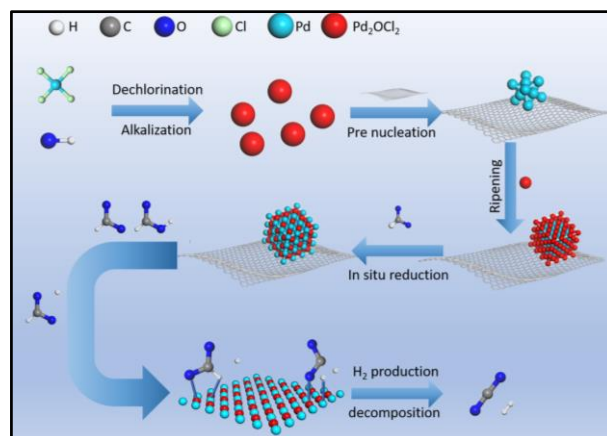
2. Results and Discussion

Preparation and Characterization

The synthesis of the catalyst is described in Scheme 1. Since the nucleation step and the in situ reduction step are separated, the characterization of the preparation should also be separated into two aspects. One aspect is the characterization of the precursor to confirm whether the pre-nucleation step could provide the ultra-small precursor crystal nucleus for the in situ reduction, and the other aspect is to confirm whether the in situ reduction step could adjust the surface electronic structure to be more suitable than the other catalysts for FAD.

Transmission Electron Microscope (TEM) graphs of both the precursor and the catalyst are shown in Figure 1a,b, which show that the pre-nucleation method could effectively decrease the size of the particle. Based on the TEM results, it was found that the average particle size was increased slightly by the in situ reduction. The reason may be that the reduction process could have cleaned up the Cl^- from the particle surface, which could lead to an increase in surface energy so that the particles become more unstable for growth. No significant growth in the particle size could be observed after in situ reduction, which

confirms the practicability and superiority of this method in particle size control. In this work, the average particle size was as small as 1.86 nm, a size that is even smaller than many particles prepared by the particle size control of the surfactant.



Scheme 1. Strategy of coupling pre-nucleation with in situ reduction for preparing Pd/C catalyst toward high speed and selectivity formic acid dehydrogenation.

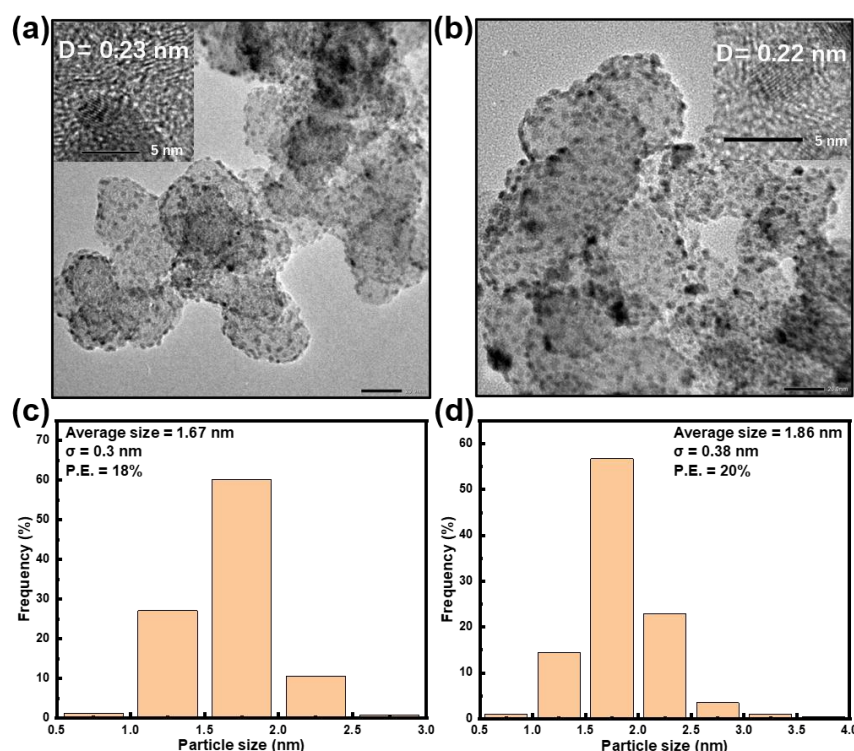


Figure 1. TEM graph for (a) pre-nucleation precursor and (b) Pd/C in situ reduction with a scale bar of 20 nm; the insert map shows the high-resolution (HR) TEM with a scale bar of 5 nm. D is the lattice spacing of the particle shown. size distribution of (c) pre-nucleation precursor and (d) Pd/C in situ reduction. the σ is the standard deviation of the particle size and the P.E. represents the percent error calculated by $\sigma/\text{average size}$.

The crystal structures of the precursor and catalyst were characterized by X-ray diffraction (XRD) and HR TEM, as shown in Figure 1a,b and Figure 2. Based on these structures, we could find that the Pd crystal existed in both samples, though the preparation of the precursor did not contain a reduction step, with only a solution alkalization to remove the coordinated Cl^- so that Pd could be anchored on the support. This confirmation could

explain the growth process of the precursor. Along with the increase in pH, the coordinated Cl^- were removed, and the Pd^{2+} coordinated with OH^- dominated the solution. Parts of these clathrates were then reduced by the reducing group on the surface of carbon support to form the crystal nucleus, which could be observed as Pd crystal in XRD, and then the other clathrates gathered to these crystal nuclei without further reduction. This conclusion could be confirmed by XRD at approximately 18 degrees in Figure 2a, which matches the (101) crystalline plane of Pd_2OCl_2 . As shown in the inset of Figure 1a,b, the precursor and the catalyst exhibit a similar lattice spacing of 0.22–0.23 nm, corresponding to the Pd(111) crystal plane (0.223 nm). However, no lattice spacing of Pd_2OCl_2 (101) ($D = 0.09$ nm) could be observed because of the demand for high resolution. This phenomenon could be used to explain why many reported Pd/Cs could not maintain an ultra-small particle size even when the surfactant was used to inhibit the growth of particles during preparation. Although the surfactant could have been adsorbed to the surface of the particles, it also blocked the contact between the Pd crystal core and those Pd clathrates in the solution, so it was difficult for the Pd solution to gather to those crystal cores to form a precursor as small as the precursor produced by this method. However, the surfactant is essential for those methods that need to reduce the Pd/C by a strong reducing agent such as NaBH_4 , as the strong reducing agent would bring strong aggregation if the surfactant is absent. These kinds of limitations could be ignored in the method suggested here, since a mild reducing agent was adopted to adjust the electronic structure of the catalyst without an obvious aggregation occurring during the reduction. In this way, surfactants could be avoided during the pre-nucleation process, and free Pd_2OCl_2 could be adsorbed to the reduced Pd(0) core to obtain precursors with ultra-small particle sizes for further in situ reduction to obtain the catalyst with the minimum particle size and most suitable electronic structure. The precursor mainly exists as Pd with high valence and a Pd(0) core, as the peak at 18 degrees in XRD disappears in the XRD of the catalyst, which has been reduced in situ, and the Pd crystal peak intensity of the precursor is much weaker than that of the reduced catalyst. The XRD of the precursor and the catalyst confirmed the structural transformation caused by the pre-nucleation and in situ reduction, while characterization of the transformation of the electronic structure should be revealed by X-ray photoelectron spectroscopy (XPS).

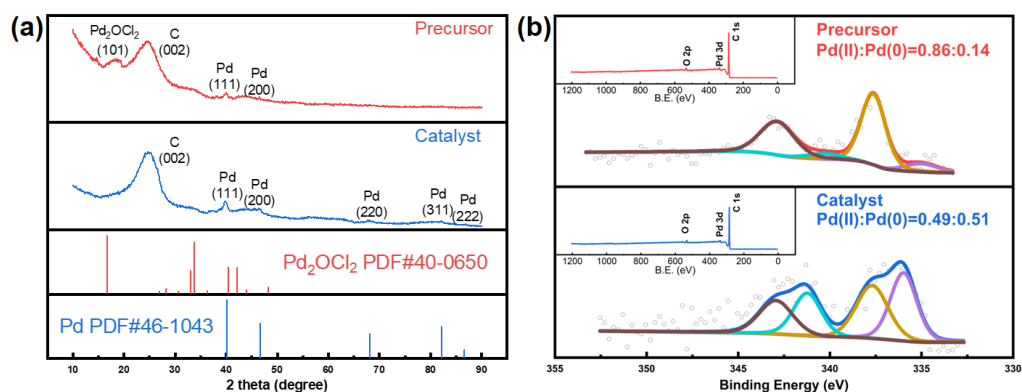


Figure 2. (a) XRD data for the pre-nucleation precursor and the catalyst by in situ reduction, along with the powder diffraction file of Pd and Pd_2OCl_2 shown by vertical lines; the scan rate is $10^\circ/\text{min}$. (b) XPS data for the pre-nucleation precursor and the catalyst by in situ reduction, along with the valence analysis and full survey.

The XPS of the precursor and the reduced catalyst is shown in Figure 2b. From Figure 2b, it is easy to conclude that the main existing form of precursor is Pd(II), along with very few of Pd(0); the ratio of Pd(II) to Pd(0) reached about 0.86:0.14, which matches the conclusion obtained from the XRD. By combining the XRD and XPS data, it is easy to confirm that the precursor is in the form of few Pd(0) crystal nuclei surrounded by the Pd(II)

clathrates. The electronic structure of the in situ reduced catalyst could also be obtained from the XPS. The ratio of Pd(II) to Pd(0) is 0.49:0.51, which is quite near to the optimum proportion of 1:1. As Pd(II) is always considered as the promoter while Pd(0) is considered as the real active site, it seems that the Pd(0)-Pd(II) could form the site for FAD.

Thus, it is easy to infer the process of the in situ reduction. The reaction starts with the traditional redox reaction, which occurs between the oxidizing Pd(II) from the precursor and the reductive carbonyl of the formate or formic acid. This reaction could be expressed as $\text{Pd}^{2+} + \text{HCOOH} = \text{Pd} + 2\text{H}^+ + \text{CO}_2$. In this way, the content of Pd(0) of the surface was increased so that more and more Pd(II)-Pd(0) sites could be formed. When the reductive formate touches these Pd(II)-Pd(0) sites, the dehydrogenation process occurs before the redox reaction, as the ortho Pd(0) shares part of the positive charge from Pd(II) to reduce the oxidability to hold up the redox reaction. Over time, more and more Pd(II) sites are reduced to form Pd(0) until nearly all of the surface is composed of Pd(II)-Pd(0) sites and the redox reaction is completely stopped. Other methods could not stop the reduction step, so the reduction could not always be controlled, and catalysts with more Pd(0) content have been prepared and reported. In this way, a final catalyst with both ultra-small particle size and adjusted electronic structure was obtained. Considering that the low Pd(II) content could lead to a lower performance of sites while the low Pd(0) content could lead to a lower mass-specific activity, conclusions which have been confirmed by several reports by the size effect and CO masking experiment, these facts could be used to explain why the catalyst with the particle size and the electronic structure in this work could exhibit excellent performance in FAD.

Evaluation of formic acid dehydrogenation has been carried out by reforming tests under a series of temperatures in Figure 3, and the evaluation of formic acid dehydration has been monitored by in situ mass spectra to determine the released CO in Figure 4.

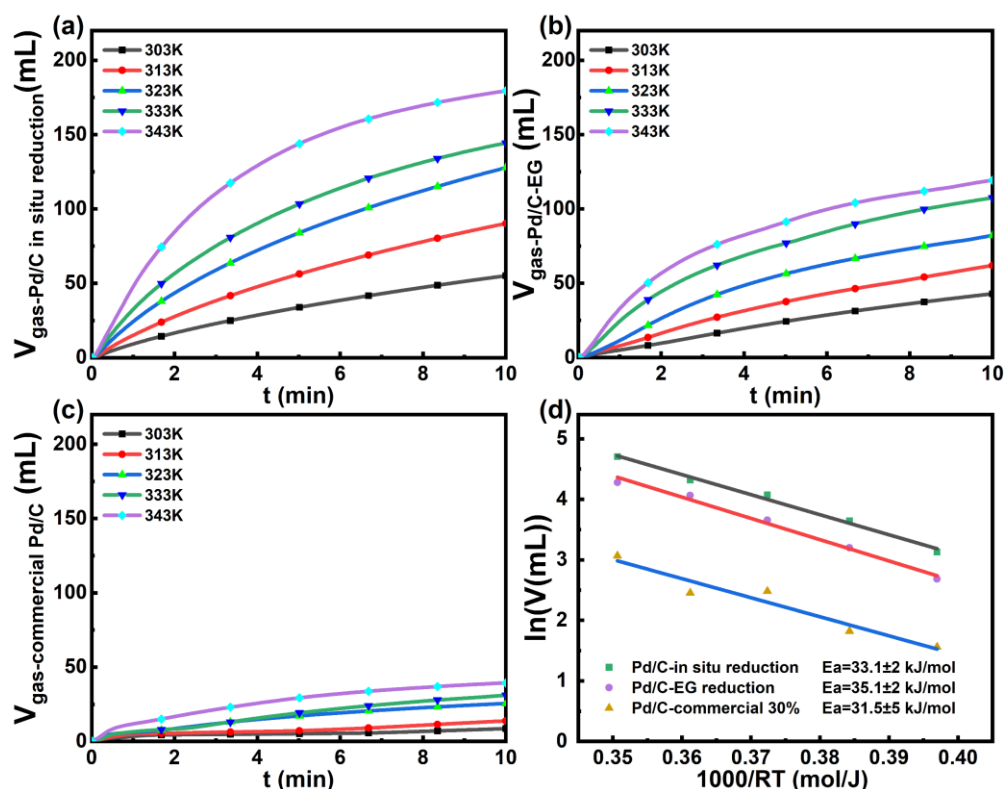


Figure 3. Time course of reforming gas evolution in 1.1 M formic acid + 0.8 M sodium formate over (a) Pd/C in situ reduction, (b) Pd/C-EG reduction, and (c) Pd/C-30% commercial; (d) analysis of the activation energy of these catalysts.

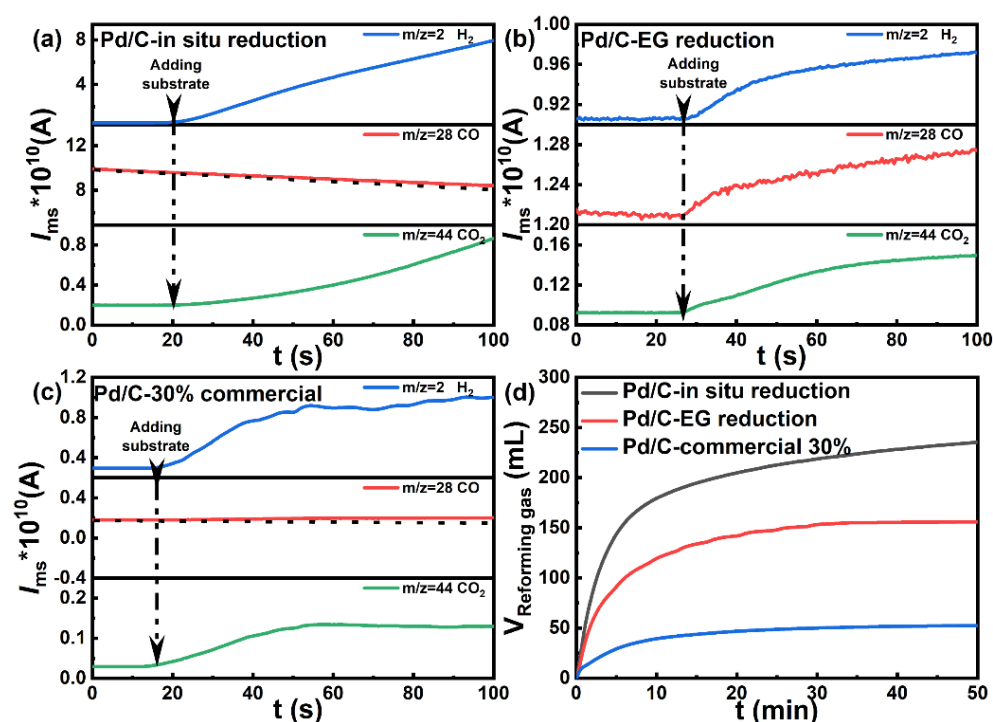


Figure 4. In situ mass spectra of the products during formic acid decomposition over (a) Pd/C in situ reduction, (b) Pd/C-EG reduction and (c) Pd/C-30% commercial; (d) Comparison of these three catalysts' performance under 343 K.

The reaction rates of the catalysts are mainly affected by the adsorption energy and desorption energy of the intermediates. The adsorption process is always disturbed by the CO from the formic acid dehydration process. The toxic molecule could block the Pd(0) sites, which makes the adsorption difficult and causes high energy loss for the desorption of CO. Fortunately, the desorption of formic acid could go on without the influence from CO and could even be accelerated by Pd(II). However, when the content of Pd(II) becomes too high, a decrease in the activity could also be observed because of the lack of Pd(0) [12]. Due to the large content of Pd(0) sites for adsorption and the large content of Pd(II) sites for desorption, the Pd/C in situ reduction could exhibit extraordinary performance in formic acid decomposition.

The difference in stability could also be explained by the above statements. From Figure 4a–c, it is easy to conclude that the yield of CO varies over different catalysts during formic acid decomposition. Due to the higher CO yield of commercial Pd/C and Pd/C-EG, these two catalysts are fully deactivated before the complete decomposition of formic acid in Figure 4d. By contrast, Pd/C in situ reduction could release about 250 mL of gas, close to the ideal yield of 270 mL, assuming the complete decomposition of formic acid and that the decrease in the rate of Pd/C in-situ reduction could be attributed to the dilute formic acid rather than the activity loss of the catalyst. The enhanced stability of the catalyst could be attributed to fewer Pd(0)-Pd(0) sites, which was considered to be the main site for dehydration by DFT calculations [26].

The decrease in activation energy (33.1 kJ/mol) could be attributed to the high density of Pd(0)-Pd(II) interface sites and the extraordinary mass-specific performance (8.94 mol_{H2}/(g_{Pd}·h)) could be attributed to the optimum valence composition with the ultra-small size, which is quite competitive with the catalysts reported in Table 1.

Table 1. Comparison of the mass-specific performance (MSP) and activation energy (Ea) between different types of reported catalysts with the catalyst prepared by coupling pre-nucleation and in situ reduction in this work.

Catalyst	MSP (mol _{H2} /(g _{Pd} ·h))	Ea (kJ/mol)	T (K)
this work	8.94	33.1	303
Pd/C [29]	1.5	\	303
Pd-B [29]	3.5	\	303
Pd@CN [28]	\	46.9	303
Ag@Pd/C [10]	0.164	30	293
Pd ₁ Au ₁ /C [21]	\	34.4	333
AuPd–MnO _x /ZIF-8-rGO [30]	1.65	\	298
PdAg–MnO _x /N-SiO ₂ [31]	1.05	\	303
Co _{0.30} Au _{0.35} Pd _{0.35} /C [22]	0.05	\	298
Pd/MS-30 [32]	3.59	\	298

3. Materials and Methods

3.1. Chemicals and Materials

Vulcan carbon powder XC-72 (Cabot Co. Boston, Massachusetts, USA), PdCl₂ (59% Pd, Shanghai Chemical Reagent Co., Ltd. Shanghai, China), formic acid (HCOOH, 97%, Alfa Aesar, Ward Hill, USA), sodium formate dehydrate (HCOONa·2H₂O, sinopharm Chemical Reagent Co., Ltd. Shanghai, China), NaOH (97%, Shanghai Aladdin Biochemical Technology Co., Ltd. Shanghai, China), and ethylene glycol (AR, XILONG SCIENTIFIC, Guangdong, China) were all used as received. Thirty percent commercial Pd/C was bought from Sigma-Aldrich (Darmstadt, Germany). Highly purified argon (≥99.99%) was supplied by Changchun Juyang Co., Ltd (Changchun, China). Ultrapure water (resistivity: ρ = 18.25 MΩ·cm⁻¹) was used to prepare the solutions. One gram PdCl₂ was dissolved into 0.1 M HCl aqueous solution to obtain H₂PdCl₄ solution.

3.2. Preparation of the Catalyst

The precursor was prepared by a simple method of precipitation to transfer the Pd atoms from the solution to the surface of the support. First, 95 mg of Vulcan XC-72 and 120 mL of ultrapure water were mixed under ultrasonic in a 250 mL beaker for 30 min, then 0.847 mL H₂PdCl₄ (5.9 mg_{Pd}/mL total 5 mg_{Pd}) was added and mixed by stirring at 500 r/min for 4 h. Subsequently, the pH of the solution was adjusted to about 10.9 by fresh 1 M NaOH solution, followed by stirring for 4h for nucleation and maturation. After filtration, the filtrate was stabilized at a pH = 7 and dried at 55 °C, and the precursor could be obtained.

The catalyst was prepared by reducing the precursor in situ. Fifty milligrams of the precursor was weighed and put into a 25 mL breaker to react with 5 mL 0.8 M HCOONa for 2 min, followed by filtration and drying to obtain the prepared catalyst.

The EG reduction method assisted by a microwave was taken for comparison. In a typical process, 237.5 mg of carbon support (XC-72) was uniformly mixed with 100 mL of ethylene glycol by ultrasonic dispersion, followed by the addition of 12.5 mg of Pd (5.9 mg_{Pd}/mL H₂PdCl₄ dissolved in 0.1 M HCl). The dispersion was stirred for 3 h for uniform mixing and pre-adsorption. Then, 1 M NaOH was used to regulate the pH of the system to a pH = 10.8. Subsequently, the microwave-assisted reduction was carried out. It should be noted that the magnetic stirrer must be taken out of the beaker before the microwave treatment for safety. The microwave treatment was done for 90 s for the first time, and subsequently for 10 s off, 10 s on, 10 s off, and 10 s on. After 8h of stirring and ripening, the obtained suspension solution was filtered and washed till the pH of filtrate was about 7. After drying in the oven at 55 °C for 12h and fully grinding the product, the target catalyst was obtained for the following tests, characterization, and analysis.

3.3. Test for Formic Acid Decomposition

The test of the formic acid decomposition was carried out in a 50 mL round-bottom flask at different temperatures under stirring, along with direct monitoring by Alicat MC serial #171607 for the recording of the total volume and mass of the reforming gas over time. Each test was carried out by reacting 20 mg of the catalyst with 5 mL of solution (1.1 M formic acid and 0.8 M sodium formate) after 10 min of Ar purging and preheating the solution.

3.4. In Situ Mass Spectra (ISMS) Test

ISMS measurements were carried out to detect the in-situ CO production during the FAD. The reforming reaction took place in a probe-type electrochemical cell, which permitted the products to be quickly captured in the detection system and ensured the sensitivity of the test. The beginning water (80 mL) was saturated with Ar. The Ar was also introduced all the time during the reaction at a flow rate of $50 \text{ mL} \cdot \text{min}^{-1}$. The end of the probe, or the injection port of the mass spectrometry system, was covered with a PTFE membrane to isolate the liquid while collecting the product. The distance between the probe end point and the catalyst was precisely controlled at about 10 microns by the lifting system. To prepare the catalyst ink, 5 mg of the catalyst was dispersed into 50 μL of Nafion (5 wt%) solution and 950 μL of ethanol by sonication for 1 h. Twenty microliters of the catalyst ink was dropped onto a glassy carbon electrode (5 mm in diameter), and the catalyst-film-coated working electrode was obtained after air-drying. The reaction starts by pouring 20 mL of the concentrated reaction solution into the beginning water. The volatile products of the reforming reactions were monitored at different values of m/z ionic signals.

3.5. Catalyst Characterization

The transmission electron microscope (TEM) images were obtained using a JEOL JEM-2800 microscope (Tokyo, Japan) operating at 200 kV with nominal resolution. Samples were sonicated and dispersed in EtOH and placed dropwise onto a holey carbon support grid for TEM observation. The X-ray diffraction (XRD) patterns were obtained using a Rigaku-D/MAX-PC 2500 X-ray diffractometer (Tokyo, Japan) with $\text{CuK} \alpha$ ($\lambda = 1.5405 \text{ \AA}$) as a radiation source, which operated at 40 kV and 200 mA. X-ray photoelectron spectroscopy (XPS) measurements were performed on a Kratos XSAM-800 spectrometer (Manchester, U.K.) with an $\text{Al K} \alpha$ radiation source.

4. Conclusions

By combining pre-nucleation and in situ reduction for the preparation of catalysts toward FAD, catalysts with high mass-specific performance ($8.94 \text{ mol}_{\text{H}_2} / (\text{g}_{\text{Pd}} \cdot \text{h})$) and low activation energy (33.1 kJ/mol) have been successfully prepared. Their performance value was 2.5 times larger than that of reported Pd-based catalysts, and the activation energy was as low as that of alloy catalysts. In situ mass spectra also confirmed the high selectivity of this catalyst.

The superb activity and selectivity of this catalyst can be attributed to the maximum number of Pd(0)-Pd(II) interface sites. The pre-nucleation could limit the particle growth effectively to expose more Pd over the surface and the in-situ reduction could adjust the ratio of Pd(II) and Pd(0) to 1:1. Using this method, the mass-specific content of Pd(0)-Pd(II) interface sites over the catalyst's surface could be maximized successfully.

The extraordinary performance of this catalyst shows that this method is promising for adjusting the specific valence composition of the catalyst with the demand for high site utilization.

Author Contributions: Conceptualization, Q.M.; methodology, Q.M. and X.Y.; formal analysis, Q.M., X.W. and K.L.; writing—original draft preparation, Q.M.; writing—review and editing, M.X., Z.J. and J.G.; project administration, C.L.; funding acquisition, C.L. and W.X. All authors have read and agreed to the published version of the manuscript.

Funding: This research was funded by the National Natural Science Foundation of China, grant number 21633008, the Instrument Developing Project of the Chinese Academy of Sciences, the Strategic Priority Research Program of the Chinese Academy of Sciences, grant number No. XDA21090400 and the Natural Science Foundation of Jilin Province, grant number 20190201300JC.

Data Availability Statement: Not applicable.

Acknowledgments: Wei Xing acknowledge Gusu Talent program for the financial support.

Conflicts of Interest: The authors declare no conflict of interest.

References

1. Li, K.; Li, Y.; Wang, Y.M.; Ge, J.J.; Liu, C.P.; Xing, W. Enhanced electrocatalytic performance for the hydrogen evolution reaction through surface enrichment of platinum nanoclusters alloying with ruthenium in situ embedded in carbon. *Energy Environ. Sci.* **2018**, *11*, 1232–1239. [[CrossRef](#)]
2. Lubitz, W.; Tumas, W. Hydrogen: An Overview. *Chem. Rev.* **2007**, *107*, 3900–3903. [[CrossRef](#)] [[PubMed](#)]
3. Midilli, A.; Ay, M.; Dincer, I.; Rosen, M.A. On hydrogen and hydrogen energy strategies I: Current status and needs. *Renew. Sustain. Energy Rev.* **2005**, *9*, 255–271. [[CrossRef](#)]
4. Eberle, U.; Felderhoff, M.; Schueth, F. Chemical and Physical Solutions for Hydrogen Storage. *Angew. Chem. Int. Ed.* **2009**, *48*, 6608–6630. [[CrossRef](#)]
5. Sordakis, K.; Tang, C.; Vogt, L.K.; Junge, H.; Dyson, P.J.; Beller, M.; Laurency, G. Homogeneous Catalysis for Sustainable Hydrogen Storage in Formic Acid and Alcohols. *Chem. Rev.* **2018**, *118*, 372–433. [[CrossRef](#)] [[PubMed](#)]
6. Palo, D.R.; Dagle, R.A.; Holladay, J.D. Methanol Steam Reforming for Hydrogen Production. *Chem. Rev.* **2007**, *107*, 3992–4021. [[CrossRef](#)] [[PubMed](#)]
7. Enthaler, S.; von Langermann, J.; Schmidt, T. Carbon dioxide and formic acid—the couple for environmental-friendly hydrogen storage? *Energy Environ. Sci.* **2010**, *3*, 1207–1217. [[CrossRef](#)]
8. Yang, L.; Li, G.; Ge, J.; Liu, C.; Jin, Z.; Wang, G.; Xing, W. TePbPt alloy nanotube as electrocatalyst with enhanced performance towards methanol oxidation reaction. *J. Mater. Chem. A* **2018**, *6*, 16798–16803. [[CrossRef](#)]
9. Wang, P.; Steinmann, S.N.; Fu, G.; Michel, C.; Sautet, P. Key Role of Anionic Doping for H₂ Production from Formic Acid on Pd(111). *ACS Catal.* **2017**, *7*, 1955–1959. [[CrossRef](#)]
10. Tedsree, K.; Li, T.; Jones, S.; Chan, C.W.A.; Yu, K.M.K.; Bagot, P.A.J.; Marquis, E.A.; Smith, G.D.W.; Tsang, S.C.E. Hydrogen production from formic acid decomposition at room temperature using a Ag-Pd core-shell nanocatalyst. *Nat. Nanotechnol.* **2011**, *6*, 302–307. [[CrossRef](#)]
11. Li, J.; Chen, W.; Zhao, H.; Zheng, X.; Wu, L.; Pan, H.; Zhu, J.; Chen, Y.; Lu, J. Size-dependent catalytic activity over carbon-supported palladium nanoparticles in dehydrogenation of formic acid. *J. Catal.* **2017**, *352*, 371–381. [[CrossRef](#)]
12. Zhang, S.; Jiang, B.; Jiang, K.; Cai, W.B. Surfactant-Free Synthesis of Carbon-Supported Palladium Nanoparticles and Size-Dependent Hydrogen Production from Formic Acid-Formate Solution. *ACS Appl. Mater. Interfaces* **2017**, *9*, 24678–24687. [[CrossRef](#)]
13. Lv, Q.; Meng, Q.; Liu, W.; Sun, N.; Jiang, K.; Ma, L.; Peng, Z.; Cai, W.; Liu, C.; Ge, J.; et al. Pd-PdO Interface as Active Site for HCOOH Selective Dehydrogenation at Ambient Condition. *J. Phys. Chem. C* **2018**, *122*, 2081–2088. [[CrossRef](#)]
14. Wang, X.; Meng, Q.L.; Gao, L.Q.; Liu, J.; Ge, J.J.; Liu, C.P.; Xing, W. Metal organic framework derived nitrogen-doped carbon anchored palladium nanoparticles for ambient temperature formic acid decomposition. *Int. J. Hydrog. Energy* **2019**, *44*, 28402–28408. [[CrossRef](#)]
15. Chen, Y.Q.; Li, X.F.; Wei, Z.Z.; Mao, S.J.; Deng, J.; Cao, Y.L.; Wang, Y. Efficient synthesis of ultrafine Pd nanoparticles on an activated N-doping carbon for the decomposition of formic acid. *Catal. Commun.* **2018**, *108*, 55–58. [[CrossRef](#)]
16. Wei, J.; Wang, H.Z.; Zhang, Q.H.; Li, Y.G. One-pot Hydrothermal Synthesis of N-Doped Carbon Quantum Dots Using the Waste of Shrimp for Hydrogen Evolution from Formic Acid. *Chem. Lett.* **2015**, *44*, 241–243. [[CrossRef](#)]
17. Kim, Y.; Kim, D. Hydrogen production from formic acid dehydrogenation over a Pd supported on N-doped mesoporous carbon catalyst: A role of nitrogen dopant. *Appl. Catal. A-Gen.* **2020**, *608*, 117887. [[CrossRef](#)]
18. Golub, F.S.; Beloshapkin, S.; Guse'nikov, A.V.; Bolotov, V.A.; Parmon, V.N.; Bulushev, D.A. Boosting Hydrogen Production from Formic Acid over Pd Catalysts by Deposition of N-Containing Precursors on the Carbon Support. *Energies* **2019**, *12*, 3885. [[CrossRef](#)]
19. Xing, Z.H.; Guo, Z.L.; Chen, X.Y.; Zhang, P.; Yang, W.S. Optimizing the activity of Pd based catalysts towards room-temperature formic acid decomposition by Au alloying. *Catal. Sci. Technol.* **2019**, *9*, 588–592. [[CrossRef](#)]
20. Li, S.J.; Zhou, Y.T.; Kang, X.; Liu, D.X.; Gu, L.; Zhang, Q.H.; Yan, J.M.; Jiang, Q. A Simple and Effective Principle for a Rational Design of Heterogeneous Catalysts for Dehydrogenation of Formic Acid. *Adv. Mater.* **2019**, *31*, 1806781. [[CrossRef](#)]
21. Hong, W.; Kitta, M.; Tsumori, N.; Himeda, Y.; Autrey, T.; Xu, Q. Immobilization of highly active bimetallic PdAu nanoparticles onto nanocarbons for dehydrogenation of formic acid. *J. Mater. Chem. A* **2019**, *7*, 18835–18839. [[CrossRef](#)]
22. Wang, Z.-L.; Yan, J.-M.; Ping, Y.; Wang, H.-L.; Zheng, W.-T.; Jiang, Q. An Efficient CoAuPd/C Catalyst for Hydrogen Generation from Formic Acid at Room Temperature. *Angew. Chem. Int. Ed.* **2013**, *52*, 4406–4409. [[CrossRef](#)] [[PubMed](#)]

23. Zhang, S.; Metin, O.; Su, D.; Sun, S. Monodisperse AgPd Alloy Nanoparticles and Their Superior Catalysis for the Dehydrogenation of Formic Acid. *Angew. Chem. Int. Ed.* **2013**, *52*, 3681–3684. [[CrossRef](#)] [[PubMed](#)]
24. Zhou, X.; Huang, Y.; Xing, W.; Liu, C.; Liao, J.; Lu, T. High-quality hydrogen from the catalyzed decomposition of formic acid by Pd–Au/C and Pd–Ag/Cw. *Chem. Commun.* **2008**, 3540, 3542.
25. Qin, Y.-L.; Wang, J.; Meng, F.-Z.; Wang, L.-M.; Zhang, X.-B. Efficient PdNi and PdNi@Pd-catalyzed hydrogen generation via formic acid decomposition at room temperature. *Chem. Commun.* **2013**, *49*, 10028–10030. [[CrossRef](#)] [[PubMed](#)]
26. Lv, Q.; Feng, L.; Hu, C.; Liu, C.; Xing, W. High-quality hydrogen generated from formic acid triggered by in situ prepared Pd/C catalyst for fuel cells. *Catal. Sci. Technol.* **2015**, *5*, 2581–2584. [[CrossRef](#)]
27. Wang, Z.-L.; Yan, J.-M.; Wang, H.-L.; Ping, Y.; Jiang, Q. Pd/C Synthesized with Citric Acid: An Efficient Catalyst for Hydrogen Generation from Formic Acid/Sodium Formate. *Sci. Rep.* **2012**, *2*, 598. [[CrossRef](#)] [[PubMed](#)]
28. Wang, Q.; Tsumori, N.; Kitta, M.; Xu, Q. Fast Dehydrogenation of Formic Acid over Palladium Nanoparticles Immobilized in Nitrogen-Doped Hierarchically Porous Carbon. *ACS Catal.* **2018**, *8*, 12041–12045. [[CrossRef](#)]
29. Jiang, K.; Xu, K.; Zou, S.; Cai, W.-B. B-Doped Pd Catalyst: Boosting Room-Temperature Hydrogen Production from Formic Acid-Formate Solutions. *J. Am. Chem. Soc.* **2014**, *136*, 4861–4864. [[CrossRef](#)] [[PubMed](#)]
30. Yan, J.M.; Wang, Z.L.; Gu, L.; Li, S.J.; Wang, H.L.; Zheng, W.T.; Jiang, Q. AuPd-MnOx/MOF-Graphene: An Efficient Catalyst for Hydrogen Production from Formic Acid at Room Temperature. *Adv. Energy Mater.* **2015**, *5*, 1500107. [[CrossRef](#)]
31. Bulut, A.; Yurderi, M.; Karatas, Y.; Say, Z.; Kivrak, H.; Kaya, M.; Gulcan, M.; Ozensoy, E.; Zahmakiran, M. MnOx-Promoted PdAg Alloy Nanoparticles for the Additive-Free Dehydrogenation of Formic Acid at Room Temperature. *Acs Catal.* **2015**, *5*, 6099–6110. [[CrossRef](#)]
32. Zhu, Q.L.; Tsumori, N.; Xu, Q. Sodium hydroxide-assisted growth of uniform Pd nanoparticles on nanoporous carbon MSC-30 for efficient and complete dehydrogenation of formic acid under ambient conditions. *Chem. Sci.* **2014**, *5*, 195–199. [[CrossRef](#)]